

Importance of subleading corrections for the Mott critical point

Patrick Sémon¹ and A.-M. S. Tremblay^{1,2}

¹*Département de physique and Regroupement québécois sur les matériaux de pointe, Université de Sherbrooke, Sherbrooke, Québec, Canada J1K 2R1*

²*Canadian Institute for Advanced Research, Toronto, Ontario, Canada M5G 1Z8*

(Received 17 October 2011; revised manuscript received 12 April 2012; published 1 May 2012)

The interaction-induced metal-insulator transition should be in the Ising universality class. Experiments on layered organic superconductors suggest instead that the observed critical endpoint of the first-order Mott transition in $d = 2$ does not belong to any of the known universality classes for thermal phase transitions. In particular, it is found that $\delta = 2$. Given the quantum nature of the two phases involved in the transition, we use dynamical mean-field theory and a cluster generalization to investigate whether the unusual exponents could arise as transient quantum behavior preceding the asymptotic critical behavior. In the cluster calculation, a canonical transformation that minimizes the sign problem in continuous-time quantum Monte Carlo calculations allows large improvements in accuracy. Our results show that there are important subleading corrections in the mean-field regime that can lead to an *apparent* exponent $\delta = 2$. Experiments on optical lattices could verify our predictions for double occupancy.

DOI: 10.1103/PhysRevB.85.201101

PACS number(s): 71.30.+h, 64.60.F-, 67.85.Lm, 71.10.Fd

Half-filled band materials should be metallic, but they are sometimes insulators.¹ This paradox was discussed by Boer and Verwey and by Peierls as early as 1937, but the first theoretical advancement came from Mott in 1949. He found that, as a function of some external parameter, it is possible to control the ratio of interaction energy to kinetic energy and drive the system through a metal-insulator transition. This Mott transition has by now been clearly identified in a few materials¹ and in optical lattices of cold atoms.^{2,3} The order parameter for the interaction-induced transition should be in the Ising universality class,⁴⁻⁶ with no breaking of translational or rotational invariance. This has been verified explicitly in the three-dimensional compound V_2O_3 .⁷

It thus came as a surprise when it was discovered that in two-dimensional layered κ -bisethylenedithio-tetrathiafulvalene (κ -(BEDT-TTF)₂X, or ET) organic superconductors,⁸ critical exponents for the Mott critical point, measured in both charge (conductivity)⁹ and spin (NMR) channels,¹⁰ did not belong either to the Ising universality classes or to any other plausible universality class for thermal phase transitions. Several proposals have appeared to explain this result. Imada *et al.*^{11,12} suggested that while the high-temperature regime is described by classical Ising exponents, there is also a continuous transition at $T = 0$ and, in between, a marginal quantum critical point that controls the observed behavior. Papanikolaou *et al.*¹³ instead started from the two-dimensional (2D) Ising universality class and argued that, away from criticality, the subleading energy exponent dominates for the conductivity over the leading order parameter exponent. The latter becomes relevant only very close to T_c . A recent experiment on thermal expansion coefficient finally, argues that the 2D Ising universality class is the correct one.¹⁴ That finding disagrees with the latest theoretical calculation¹⁵ performed with cluster dynamical mean-field theory (CDMFT)^{16,17} that measured an exponent $\delta = 2$, in agreement with the above-mentioned conductivity⁹ and NMR experiments.¹⁰

Here we revisit the critical behavior at the Mott critical endpoint by studying the one-band Hubbard model, the simplest model of interacting electrons that contains the physics of the

Mott transition. Given the quantum nature of the two phases involved in the transition, we investigate whether unique exponents could arise as transient quantum behavior preceding the asymptotic critical behavior. Such a quantum critical point controlling the behavior over a wide range of finite temperature has already been observed for the conductivity.¹⁸ Since the sizes of the crossover regions are not universal quantities, we need a quantitative method that accurately takes into account the quantum mechanics of this problem. To date, dynamical mean-field theory (DMFT)¹⁹⁻²¹ and cluster generalizations are the only available methods that satisfy this requirement. Single-site DMFT is exact in infinite dimension and can be applied to lower-dimensional lattices.^{22,23} CDMFT takes into account some momentum dependence of the self-energy, a physical ingredient that is known to be important in two dimensions.²⁴⁻³⁵ Hence, CDMFT should provide an accurate description of the Mott transition, except in the asymptotic regime where spatial critical fluctuations become important. To interpret our results, we also found it necessary to perform single-site DMFT calculations, for which analytical results are available.^{5,36}

Improvements in computer performance and in algorithms allow us to obtain much more accurate data than earlier calculations. In the case of CDMFT, for the frustrated lattice considered here, the sign problem in the continuous time quantum Monte Carlo solution of the hybridization expansion (CT-HYB)³⁷⁻⁴⁰ is minimized by a canonical transformation. This allows us to approach the critical point ten times closer in reduced pressure than previously possible.

Method. The simplest model that contains both the strong on-site Coulomb repulsion and the kinetic energy of the frustrated κ -ET's lattice is the half-filled Hubbard model on a 2D anisotropic triangular lattice,

$$H = \sum_{ij\sigma} (t_{ij} - \delta_{ij}\mu) c_{i\sigma}^\dagger c_{j\sigma} + U \sum_i n_{i\uparrow} n_{i\downarrow}, \quad (1)$$

where $c_{i\sigma}^\dagger$ creates a spin σ electron at site i , $n_{i\sigma} = c_{i\sigma}^\dagger c_{i\sigma}$ is the spin σ density at site i , $t_{ij} = t_{ji}^*$ are the hopping amplitudes as

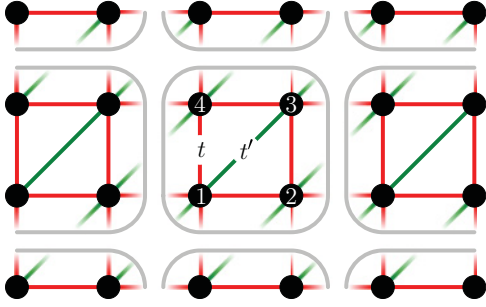


FIG. 1. (Color online) Periodic partitioning of the anisotropic triangular lattice into 2×2 plaquettes for CDMFT.

shown in Fig. 1 while μ and U are, respectively, the chemical potential and the screened Coulomb repulsion.

We use single-site DMFT²² and its cluster extension CDMFT^{16,17} to solve the Hamiltonian Eq. (1). These methods start with a periodic partitioning of the infinite lattice model into independent sites (DMFT) or clusters (CDMFT). The missing environment of the cluster is replaced by a bath of noninteracting electrons. The action of the cluster in a bath model may be written as

$$S = S_{\text{cl}}(\mathbf{c}^\dagger, \mathbf{c}) + \int_0^\beta d\tau d\tau' \mathbf{c}^\dagger(\tau') \mathbf{\Delta}(\tau' - \tau) \mathbf{c}(\tau), \quad (2)$$

where S_{cl} is the cluster action as obtained by the partitioning, \mathbf{c} the column vector of the corresponding $c_{i\sigma}$'s, and the bath has been integrated out in favor of a hybridization function $\mathbf{\Delta} = (\Delta_{i\sigma, j\sigma'})$. This defines an effective impurity model. Approximating the unknown lattice self-energy locally by the impurity self-energy, the requirement that the projection of the lattice Green's function on the cluster coincides with the impurity Green's function computed from the action Eq. (2) then self-consistently determines $\mathbf{\Delta}$. For CDMFT we take the 2×2 plaquette illustrated in Fig. 1. This accounts for the geometrical frustration in the κ -ET.

To obtain the impurity Green's function (and other observables), we use a continuous time quantum Monte Carlo (CTQMC) solver based on the expansion of the impurity action in the hybridization function.³⁷⁻⁴⁰ In the case of CDMFT, symmetries of the problem can be used to speed up the simulation by choosing a single-particle basis in Eq. (2) that transforms according to the irreducible representations.⁴⁰ In our case, separate charge conservation of $\sigma = \uparrow, \downarrow$ particles and the C_{2v} point group symmetry of the anisotropic plaquette lead to the single-particle basis (see Fig. 1 for indices),

$$\begin{aligned} c_{A_1\sigma} &= \frac{1}{\sqrt{2}}(c_{1\sigma} + c_{3\sigma}), & c'_{A_1\sigma} &= \frac{1}{\sqrt{2}}(c_{2\sigma} + c_{4\sigma}), \\ c_{B_1\sigma} &= \frac{1}{\sqrt{2}}(c_{1\sigma} - c_{3\sigma}), \\ c_{B_2\sigma} &= \frac{1}{\sqrt{2}}(c_{2\sigma} - c_{4\sigma}), \end{aligned} \quad (3)$$

with A_1 , B_1 , and B_2 irreducible representations of C_{2v} (A_2 is empty). Due to the degeneracy in the A_1 subspace, there is a degree of freedom in the choice of basis which may be parametrized by an angle θ as follows:

$$\cos\theta c'_{A_1\sigma} - \sin\theta c_{A_1\sigma}, \quad \sin\theta c'_{A_1\sigma} + \cos\theta c_{A_1\sigma}. \quad (4)$$

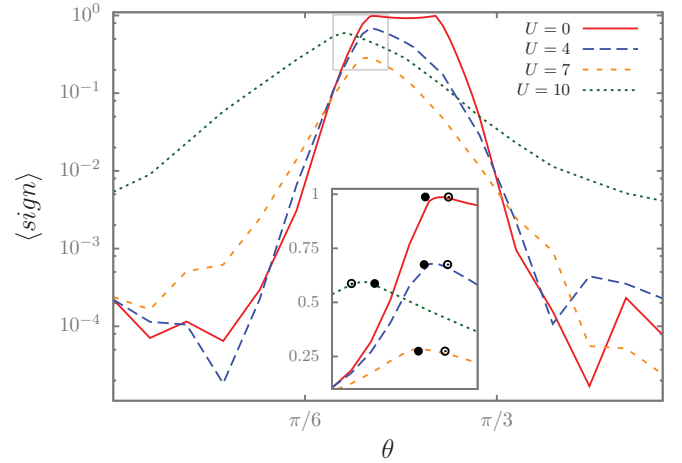


FIG. 2. (Color online) Average sign in CTQMC simulations of the anisotropic plaquette impurity problem at CDMFT self-consistency with $t/t' = 0.8$ ($t \equiv 1$) and $\beta = 20$ as a function of the angle θ in Eq. (4) for different values of U . The inset zooms on the region where the sign takes its maximum, as indicated. The dots associated with each curve indicate the angle where the off-diagonal elements of the corresponding hybridization functions are minimal with respect to the L_1 norm (solid) and the L_2 norm (empty).

In this basis the hybridization function $\mathbf{\Delta}$ takes a block-diagonal form with one 2×2 block (A_1) and two 1×1 blocks (B_1 and B_2) for each spin (in the normal phase). The sign problem in the Monte Carlo simulation shows a strong dependence in θ , as shown in Fig. 2 for $t/t' = 0.8$, $\beta = 20$, and different values of U . One can check that the maximum of the average sign is related to the angle θ that minimizes the off-diagonal elements of the hybridization function (A_1 block) with respect to some norm. The dots in the inset of Fig. 2 indicate the maximum with respect to L_1 and L_2 on $[0, \beta]$. The usual basis, $\theta = 0$, has a bad sign problem.

Results. Figure 3(a) displays double occupancy $D \equiv \langle n_\uparrow n_\downarrow \rangle$ as a function of interaction strength calculated for both single-site DMFT (blue squares) and CDMFT (red circles) at our best estimate of the corresponding critical T . Both the metallic (solid symbols) and insulating (open symbols) sides are shown. The critical temperature is found as follows. Below the critical temperature, there is hysteresis and a jump in double occupancy. Above the critical temperature, double occupancy is continuous. First we searched for the highest (lowest) temperature where hysteresis (continuity) can be checked in a reasonable time. The mean of these two temperatures is then taken as an approximation for the critical temperature.

To check for quantum transient behavior we first fit the results with $D - D_c = c \text{sgn}(U - U_c) |U - U_c|^{1/\delta}$ and different c 's on both sides. This yields $\delta \sim 2$ for DMFT and $\delta \gtrsim 2$ for CDMFT. If we restrict the fit to an interval closer to the transition, the exponent increases toward $\delta = 3$, as expected in mean-field theory. From this point of view, it is tempting to associate $\delta = 2$ to transient quantum behavior. There is an alternate possibility. In single-site DMFT we know analytically^{5,36} that δ takes its mean-field value $\delta = 3$ and that there are subleading corrections to mean field. To investigate this possibility, we first derive the subleading corrections.

The singular part of the mean-field equation for the order parameter η takes the form^{5,36}

$$p\eta + c\eta^3 = h, \quad (5)$$

with c a constant, while p and h are defined by $p \equiv p_1(U - U_c) + p_2(T - T_c)$ and $h \equiv h_1(U - U_c) + h_2(T - T_c)$. As in the liquid-gas transition, interaction strength and temperature are not in general eigendirections, which explains the way they appear in p and h . When $p = 0$, the solution is $\eta = (h/c)^{1/\delta}$, which defines $\delta = 3$. Approaching the critical line along $\delta U \equiv (U - U_c)$ for example, the mean-field Eq. (5) takes the form

$$p_1\delta U\eta + c\eta^3 = h_1\delta U. \quad (6)$$

One can show that the general solution of that equation is of the form

$$\eta = \sum_{i=1}^{\infty} \delta U^{i/3} \eta_i, \quad (7)$$

with expansion coefficients η_i . The first term, $\delta U^{1/3}$, and the subleading correction, $\delta U^{2/3}$, are the only terms that lead to an infinite first derivative at the critical point. In the case of DMFT, η is the singular part of the hybridization function. Double occupancy in general should be a smooth function of η that can be expanded as a power series, a result that can be proven in DMFT.⁵ Hence, even when η is dominated by the leading term $\delta U^{1/\delta}$, the η^2 term of the power series leads to subleading $\delta U^{2/\delta}$ corrections.

The above results suggest that the data for double occupancy should be fitted with the functional form

$$D - D_c = c_1 \operatorname{sgn}(\delta U) |\delta U|^{1/\delta} + c_2 |\delta U|^{2/\delta} + c_3 \delta U, \quad (8)$$

where δ and the coefficients are adjustable parameters. The linear term proportional to c_3 is nonsingular and is present on general grounds. When a linear term is added to the $\delta = 2$ fits above, the number of fit parameters is identical to here, and the results are unchanged. Here we find that with the subleading corrections and the linear term, it is possible to obtain an excellent fit to all the points in Fig. 3. In addition, the fit parameters, including the exponent, are insensitive to the range of the fit. This robustness of the fit and the better quality of the fits demonstrate that the alternative quantum transient hypothesis must be rejected. The solid lines are fits to the functional form suggested by Eq. (8) and by the smoothness hypothesis for D . The fits include both the metallic and the insulating sides. We find $\delta = 2.93 \pm 0.15$ for DMFT, where we know that the analytical result⁵ asymptotically is $\delta = 3$. For CDMFT we find $\delta = 3.04 \pm 0.25$. The error in the fitting parameter δ , estimated as described in Ref. 41, is small compared to the one caused by the uncertainty in the critical temperature. We therefore estimate the errors from the values of δ at the two temperatures just below and above the critical one. The log-log plot in Fig. 3(b) shows that the data does not lie on a perfect straight line over the wide range of reduced units considered here. The straight dashed lines are guides to the eye that show that the exponent that we would obtain by fitting over a limited range of δU would decrease from $\delta = 3$ toward $\delta = 3/2$ as we move away from the critical point. On

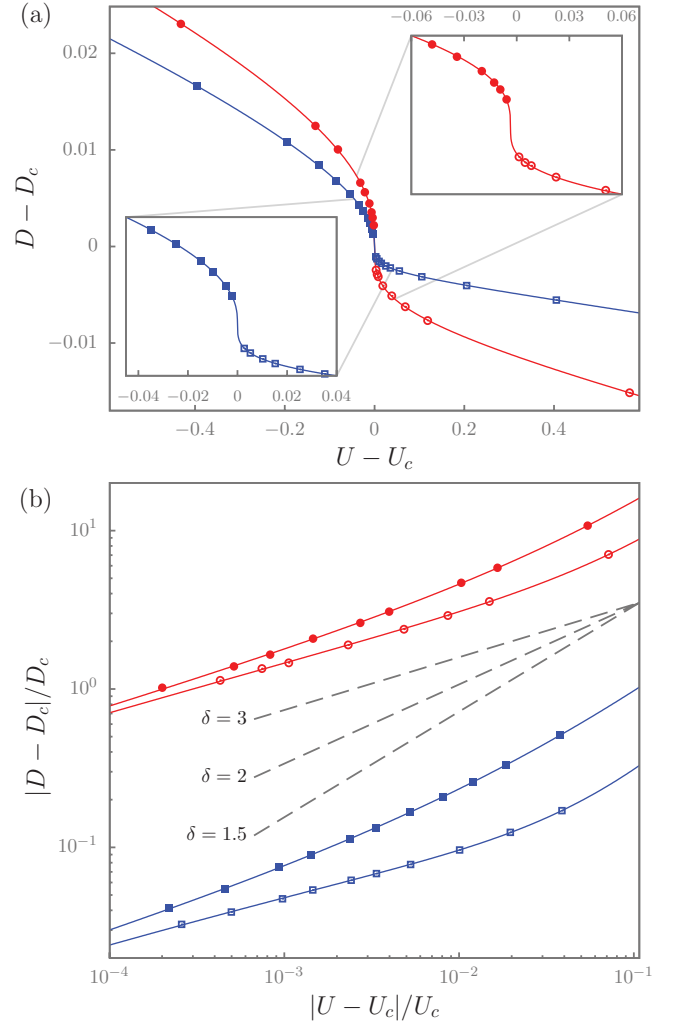


FIG. 3. (Color online) Double occupancy as a function of U near the Mott critical point for the Hubbard model on an anisotropic triangular lattice with $t'/t = 0.8$ ($t \equiv 1$) at half filling and fixed critical inverse temperature $\beta = 11.15$ (squares) for DMFT and $\beta = 9.9$ (circles, shifted by $\times 10^{1.5}$) for CDMFT on a 2×2 plaquette. The solid lines show a fit to $f(U) = c_1 \operatorname{sgn}(\delta U) |\delta U|^{1/\delta} + c_2 |\delta U|^{2/\delta} + c_3 \delta U + D_c$ ($\delta U \equiv U - U_c$) with the same parameters c_1, c_2, c_3, D_c, U_c , and δ for the metallic (filled symbols) and the insulating region (open symbols). The best fitting values (U_c, D_c, δ) are (10.445, 0.0325, 2.93) for DMFT and (7.932, 0.0679, 3.04) for CDMFT. (a) Linear plot centered at (U_c, D_c) . The insets zoom on the regions close to the critical point. (b) Logarithmic plot in reduced units relative to the critical point with CDMFT data shifted by a factor of $10^{1.5}$ along the y axis. The dashed lines show the function $\propto |U - U_c|^{1/\delta}$ with δ as indicated. In the critical regime, up to 500 iterations are necessary for convergence in the iterative solution of the (C)DMFT equation. Once convergence is reached, we take the average over hundreds of iterations. Monte Carlo sweeps per iteration: 6×10^9 for DMFT and 10^9 for CDMFT.

the metallic side, the crossover extends over a rather wide region where δ is close to $\delta = 2$.

As shown in Table I, different critical quantities lead to coherent estimates of δ , whereas the importance of the subleading corrections varies strongly from case to case. For

TABLE I. Estimates of the exponent δ from a fit of Eq. (8) to the critical behavior of the double occupancy D , the local Green's function G_{loc} at $\tau = \beta/2$, and the real and imaginary parts of the local hybridization Δ_{loc} function at the lowest Matsubara frequency, as obtained by DMFT and CDMFT for the same model and parameters as in Fig. 3. The ratio $|c_2/c_1|$ indicates the weight of the subleading correction, as seen from Eq. (8). The error for δ is ± 0.25 for CDMFT and ± 0.15 for DMFT.

	DFMT		CDMFT	
	δ	$ c_2/c_1 $	δ	$ c_2/c_1 $
D	2.93	1.15	3.04	0.51
$G_{\text{loc}}(\tau = \beta/2)$	2.99	0.32	3.05	0.33
$\text{Im}\Delta_{\text{loc}}(\omega_n = \pi/\beta)$	3.02	0.28	3.08	0.086
$\text{Re}\Delta_{\text{loc}}(\omega_n = \pi/\beta)$	2.87	0.79	3.02	0.75

the single-band Hubbard model, the singular behavior of D implies singular behavior in both spin and charge channels,⁵ as follows from the following two sum rules on spin, χ_{sp} , and charge, χ_{ch} , susceptibilities, $T \sum_n \int \frac{d^2q}{(2\pi)^2} \chi_{\text{sp}}(\mathbf{q}, \omega_n) = n - 2D$ and $T \sum_n \int \frac{d^2q}{(2\pi)^2} \chi_{\text{ch}}(\mathbf{q}, \omega_n) = n + 2D - n^2$, where ω_n are Matsubara frequencies and \mathbf{q} wave vectors in the Brillouin zone.

Below the critical temperature, there is a first-order transition with a jump in double occupancy that scales as p^β with $\beta = 1/2$. It is very difficult to obtain this exponent numerically because of hysteresis. Similarly, the exponent for the susceptibility $(\partial\eta/\partial h)_p \sim p^{-\gamma}$ with $\gamma = 1$ requires numerical differentiation and cannot be obtained accurately.

Discussion. Fitting with a single exponent over a broad region away from the critical point leads to $\delta \approx 2$,¹⁵ as observed experimentally.^{9,10} Hence it is tempting to interpret this result as a quantum mechanical transient behavior. However, the fact that $\delta \approx 2$ is obtained also for single-site DMFT, where analytical results exist,⁵ leads us instead to look at the alternate hypothesis that subleading corrections to mean-field theory explain the results. With the same number of parameters in both kinds of fits, we find with subleading corrections that $\delta = 3$ gives a much better agreement with all the data for both

DMFT and CDMFT. Subleading corrections are particularly important when the accessible data is asymmetric about the critical point.

Extracting the pressure dependence of model parameters from band-structure calculations,⁴² we estimate that our numerical results are as close to the critical point in reduced units as are the experiments. The value $\gamma = 1$ in these experiments is the same as the mean-field one, while $\beta = 1$ would imply that a nonsingular term dominates the physics in the accessible range.

Our results could be relevant for experiment if the failure of mean-field theory due to long-wavelength fluctuations occurs only very close to the critical point. Here, the size of the critical region, as determined from the Ginzburg criterion, is not known. A sizeable mean-field regime has been obtained experimentally for the 3D Mott transition.⁷ Mean-field behavior could also be observed because of coupling to the lattice.⁴³ This case would also lead to subleading corrections with the same exponents but different sizes of the crossover regions. It would thus be interesting to reanalyze the experimental results by including the subleading correction to the mean-field behavior.

To definitely settle this issue experimentally, it would be interesting to study the two-dimensional Mott transition in frustrated optical lattices, where double occupancy is directly accessible.²

Acknowledgments. We are indebted to D. Sénéchal, C. Bourbonnais, J. Schmalian, R. Fernandes, E. Fradkin, M. Sentef, and E. Gull for useful discussions. This work was partially supported by NSERC, the Tier I Canada Research Chair Program (A.-M.S.T.), and Université de Sherbrooke. A.-M.S.T. is grateful to the Harvard Physics Department for support and P. Sémon for hospitality during the writing of this work. Partial support was also provided by the MIT-Harvard Center for Ultracold Atoms. Simulations were performed using a code based on the ALPS library⁴⁴ on computers provided by CFI, MELS, Calcul Québec, and Compute Canada. Portions of the hybridization expansion impurity solver developed by P. Sémon were inspired by the code graciously provided by E. Gull and P. Werner.

¹M. Imada, A. Fujimori, and Y. Tokura, *Rev. Mod. Phys.* **70**, 1039 (1998).

²R. Jordens, N. Strohmaier, K. Gunter, H. Moritz, and T. Esslinger, *Nature (London)* **455**, 204 (2008).

³U. Schneider, L. Hackermüller, S. Will, T. Best, I. Bloch, T. A. Costi, R. W. Helmes, D. Rasch, and A. Rosch, *Science* **322**, 1520 (2008).

⁴C. Castellani, C. DiCastro, D. Feinberg, and J. Ranninger, *Phys. Rev. Lett.* **43**, 1957 (1979).

⁵G. Kotliar, E. Lange, and M. J. Rozenberg, *Phys. Rev. Lett.* **84**, 5180 (2000).

⁶S. Onoda and N. Nagaosa, *J. Phys. Soc. Jpn.* **72**, 2445 (2003).

⁷P. Limelette, A. Georges, D. Jerome, P. Wzietek, P. Metcalf, and J. M. Honig, *Science* **302**, 89 (2003).

⁸S. Lefebvre, P. Wzietek, S. Brown, C. Bourbonnais, D. Jérôme, C. Mézière, M. Fourmigué, and P. Batail, *Phys. Rev. Lett.* **85**, 5420 (2000).

⁹F. Kagawa, K. Miyagawa, and K. Kanoda, *Nature (London)* **436**, 534 (2005).

¹⁰F. Kagawa, K. Miyagawa, and K. Kanoda, *Nat. Phys.* **5**, 880 (2009).

¹¹M. Imada, *Phys. Rev. B* **72**, 075113 (2005).

¹²M. Imada, T. Misawa, and Y. Yamaji, *J. Phys.: Condens. Matter* **22**, 164206 (2010).

- ¹³S. Papanikolaou, R. M. Fernandes, E. Fradkin, P. W. Phillips, J. Schmalian, and R. Sknepnek, *Phys. Rev. Lett.* **100**, 026408 (2008).
- ¹⁴L. Bartosch, M. de Souza, and M. Lang, *Phys. Rev. Lett.* **104**, 245701 (2010).
- ¹⁵M. Sentef, P. Werner, E. Gull, and A. P. Kampf, *Phys. Rev. B* **84**, 165133 (2011).
- ¹⁶G. Kotliar, S. Y. Savrasov, G. Pálsson, and G. Biroli, *Phys. Rev. Lett.* **87**, 186401 (2001).
- ¹⁷T. Maier, M. Jarrell, T. Pruschke, and M. H. Hettler, *Rev. Mod. Phys.* **77**, 1027 (2005).
- ¹⁸H. Terletska, J. Vučićević, D. Tanasković, and V. Dobrosavljević, *Phys. Rev. Lett.* **107**, 026401 (2011).
- ¹⁹W. Metzner and D. Vollhardt, *Phys. Rev. Lett.* **62**, 324 (1989).
- ²⁰A. Georges and G. Kotliar, *Phys. Rev. B* **45**, 6479 (1992).
- ²¹M. Jarrell, *Phys. Rev. Lett.* **69**, 168 (1992).
- ²²A. Georges, G. Kotliar, W. Krauth, and M. J. Rozenberg, *Rev. Mod. Phys.* **68**, 13 (1996).
- ²³G. Kotliar, S. Y. Savrasov, K. Haule, V. S. Oudovenko, O. Parcollet, and C. A. Marianetti, *Rev. Mod. Phys.* **78**, 865 (2006).
- ²⁴A. I. Lichtenstein and M. I. Katsnelson, *Phys. Rev. B* **62**, R9283 (2000).
- ²⁵O. Parcollet, G. Biroli, and G. Kotliar, *Phys. Rev. Lett.* **92**, 226402 (2004).
- ²⁶T. A. Maier, M. Jarrell, T. C. Schulthess, P. R. C. Kent, and J. B. White, *Phys. Rev. Lett.* **95**, 237001 (2005).
- ²⁷B. Kyung, S. S. Kancharla, D. Sénéchal, A.-M. S. Tremblay, M. Civelli, and G. Kotliar, *Phys. Rev. B* **73**, 165114 (2006).
- ²⁸B. Kyung and A.-M. S. Tremblay, *Phys. Rev. Lett.* **97**, 046402 (2006).
- ²⁹K. Haule and G. Kotliar, *Phys. Rev. B* **76**, 104509 (2007).
- ³⁰S. S. Kancharla, B. Kyung, D. Sénéchal, M. Civelli, M. Capone, G. Kotliar, and A.-M. S. Tremblay, *Phys. Rev. B* **77**, 184516 (2008).
- ³¹T. Ohashi, T. Momoi, H. Tsunetsugu, and N. Kawakami, *Phys. Rev. Lett.* **100**, 076402 (2008).
- ³²S. Sakai, Y. Motome, and M. Imada, *Phys. Rev. Lett.* **102**, 056404 (2009).
- ³³A. Liebsch and N.-H. Tong, *Phys. Rev. B* **80**, 165126 (2009).
- ³⁴A. Liebsch, H. Ishida, and J. Merino, *Phys. Rev. B* **79**, 195108 (2009).
- ³⁵G. Sordi, K. Haule, and A. M. S. Tremblay, *Phys. Rev. Lett.* **104**, 226402 (2010).
- ³⁶G. Kotliar, *Eur. Phys. J. B* **11**, 27 (1999).
- ³⁷P. Werner, A. Comanac, L. deMedici, M. Troyer, and A. J. Millis, *Phys. Rev. Lett.* **97**, 076405 (2006).
- ³⁸P. Werner and A. J. Millis, *Phys. Rev. B* **74**, 155107 (2006).
- ³⁹E. Gull, A. J. Millis, A. I. Lichtenstein, A. N. Rubtsov, M. Troyer, and P. Werner, *Rev. Mod. Phys.* **83**, 349 (2011).
- ⁴⁰K. Haule, *Phys. Rev. B* **75**, 155113 (2007).
- ⁴¹W. H. Press, S. A. Teukolsky, W. T. Vetterling, and B. P. Flannery, *Numerical Recipes in Fortran. The Art of Scientific Computing* (Cambridge University Press, Cambridge, U.K., 1992), 2nd ed., Chap. 15.6.
- ⁴²H. C. Kandpal, I. Opahle, Y.-Z. Zhang, H. O. Jeschke, and R. Valentí, *Phys. Rev. Lett.* **103**, 067004 (2009).
- ⁴³T. Chou and D. R. Nelson, *Phys. Rev. E* **53**, 2560 (1996).
- ⁴⁴A. Albuquerque *et al.*, *J. Magn. Magn. Mater.* **310**, 1187 (2007).